Journal Pre-proof

GaN/AlN Multiple Quantum Wells grown by Molecular Beam Epitaxy: Effect of growth kinetics on radiative recombination efficiency

Chirantan Singha , Sayantani Sen , Alakananda Das ,
Anirban Saha , Pallabi Pramanik , Sudipta Bera ,
Rupa Mukhopadhyay , Anirban Bhattacharyya

PII: S0040-6090(20)30425-9
DOI: https://doi.org/10.1016/j.tsf.2020.138216
Reference: TSF 138216

To appear in: *Thin Solid Films*

Received date: 5 November 2019
Revised date: 30 June 2020
Accepted date: 1 July 2020

Please cite this article as: Chirantan Singha , Sayantani Sen , Alakananda Das , Anirban Saha , Pallabi Pramanik , Sudipta Bera , Rupa Mukhopadhyay , Anirban Bhattacharyya , GaN/AlN Multiple Quantum Wells grown by Molecular Beam Epitaxy: Effect of growth kinetics on radiative recombination efficiency, *Thin Solid Films* (2020), doi: https://doi.org/10.1016/j.tsf.2020.138216

This is a PDF file of an article that has undergone enhancements after acceptance, such as the addition of a cover page and metadata, and formatting for readability, but it is not yet the definitive version of record. This version will undergo additional copyediting, typesetting and review before it is published in its final form, but we are providing this version to give early visibility of the article. Please note that, during the production process, errors may be discovered which could affect the content, and all legal disclaimers that apply to the journal pertain.

© 2020 Published by Elsevier B.V.

Highlights

- GaN/AlN Multiple Quantum Wells were grown by Molecular Beam Epitaxy
- For high III/V ratio Internal quantum efficiency (IQE) was below 10%
- For reduced III/V ratio IQE was ~28% even for high dislocation densities
- Reduction of III/V ratio generated faceted surfaces
- Spontaneously grown nanostructures observed

Journal Pre-proof

* Tel: +91 9903212063

Corresponding Author: anirban.rpe@caluniv.ac.in (A. Bhattacharyya)

GaN/AlN Multiple Quantum Wells grown by Molecular Beam Epitaxy: Effect of growth kinetics on radiative recombination efficiency

Chirantan Singha[a], Sayantani Sen[a], Alakananda Das[b], Anirban Saha[b], Pallabi Pramanik[a], Sudipta Bera[c], Rupa Mukhopadhyay[c], Anirban Bhattacharyya[b*]

[a] *Centre for Research in Nanoscience and Nanotechnology, University of Calcutta, JD2 Sector III Salt Lake City, Kolkata-700106, West Bengal, India*

[b] *Institute of Radio Physics and Electronics, University of Calcutta, 92 A. P. C. Road, Kolkata-700009, West Bengal, India*

[c] *School of Biological Sciences, Indian Association for the Cultivation of Science, Kolkata 700032, India*

Journal Pre-proof

Abstract:

Ultraviolet (UV) optoelectronic devices based on binary GaN quantum wells have been widely reported in the literature. The internal quantum efficiency (IQE) of such structures is relatively low due to the large dislocation densities generated during heteroepitaxial deposition on to non lattice-matched substrates. Enhancement of IQE is possible through the use of expensive lattice-matched substrates or by using complex dislocation density reducing mechanisms. In this paper we have investigated growth mechanisms of GaN/AlN multiple quantum wells (MQWs) using Plasma Assisted Molecular Beam Epitaxy. Specifically the modulation of the surface diffusivity of adatoms has been carried out through choice of appropriate growth parameters, such as the group-III to group-V flux ratio. Our results indicate that this leads to modification of not only the surface morphology, but also the abruptness of the well-barrier interface. Under conditions of growth where surface morphology was atomically flat, the interfaces are relatively diffuse. The IQE for such structures, as measured by the ratio of room temperature photoluminescence intensity to that measured at 4 K, is rather low typically ~10%. Use of near stoichiometric growth conditions however lead to a reduction of the surface diffusivity of adatoms, and the formation of spontaneous nanostructures in the form of nano-dots of about 20 nm in diameter and high levels of uniformity. The IQE for GaN/AlN MQWs grown under such conditions is increased to as high as 28% even for samples with large dislocation densities. Thus, growth under such conditions can mitigate the detrimental effects of non-radiative recombination centers associated with dislocations by spatial localization of electron-hole pairs. These results are important to many applications, including UV light emitting diodes.

Keywords: Molecular Beam Epitaxy, Group-III Nitrides, Binary Multiple Quantum wells, Internal Quantum efficiency.

1. Introduction:

Ultraviolet (UV) solid state sources based on III-Nitride materials are expected to play a very significant role in water purification, direct line-of-sight communications, solid state lighting, polymer curing as well as in the biomedical field. Light emitting diodes (LEDs) have been developed for wavelengths ranging from 390 nm down to 230 nm and lower, and some of these are available commercially. These devices are typically based on AlGaN alloys with different alloy compositions. However, the science behind the UV emission mechanisms in AlGaN nanoheterostructures is still not fully understood, specially due to various alloy phenomena that have been reported by several groups [1-2]. Specifically, the presence of potential fluctuations due to nanoscale compositional inhomogeneity plays a very significant role in the optical processes for AlGaN films. It has been reported that this leads to a broadening of the peak, as well as considerable red-shift. Furthermore, the band-realignment of AlGaN alloys, as reported both experimentally as well as from theoretical calculations, introduces an additional complexity [3]. Moreover, these are also specific to the deposition technique and process parameters, making it difficult to establish a clear picture accounting for the various observed results. For growth by Plasma-Assisted Molecular Beam Epitaxy (PA-MBE), these parameters include the arrival and desorption rates of the various species, the substrate temperature, and the plasma activation conditions, all of which leads to a variation of the group III to group V flux ratio. Our recently published results on Multiple Quantum Well (MQW) structures with AlGaN both in the wells and the barriers indicate that this particular parameter has a strong impact on the structural, interfacial and luminescence properties, specifically the internal quantum efficiency (IQE) [4]. A major reason lies in the variation of surface mobility and desorption rates of Al and Ga adatoms, which under certain conditions allow the deliberate incorporation of compositional

Journal Pre-proof

inhomogeneities, leading to improved radiative recombination rates. However, the well-barrier interface quality is reduced, and necessitates the incorporation of additional process steps in order to generate abrupt interfaces.

Use of GaN as the well material can help to significantly lower the impact of these phenomena, thereby simplifying the process steps. UV LEDs emitting at ~350 nm employing GaN quantum wells have been reported [5]. GaN/AlN MQWs have been used for UV generation by e-beam excitation for wavelengths as low as 235 nm and power levels as high as 150 mW has been reported [6]. The efficiency of these structures has been determined both by direct measurements as well as by temperature dependent photoluminescence (PL) measurements. The reported values of IQE depend strongly on the level of dislocation densities [7-8]. For Metal Organic Chemical Vapour Deposition grown samples on sapphire, while IQE values as low as 0.18% to 0.39% have been reported [9], for lower dislocation densities [10] of few 10^9 cm^{-2} it increased to 26%. This is in line with the theoretical calculations [11] where the IQE is expected to reduce from 95% to below 5% as the dislocation densities increase from 1×10^7 cm^{-2} to 1×10^{10} cm^{-2}. Takeda et al. have employed Lateral Epitaxial Overgrowth techniques on patterned templates [12] to increase IQE values from 5% up to 45% by reducing dislocation densities of 4×10^9 cm^{-2} to 2×10^8 cm^{-2}.

Another source of loss of IQE is the presence of built-in electric fields in MQWs grown along the (0001) direction [13-14], which cause quantum confined stark effect (QCSE), separating the electron and hole wave functions and reducing radiative recombination probability. This can be avoided by growth along non-polar and semi-polar directions, but this requires deposition on to non-standard substrates. Incorporation of an additional AlGaN layer between wells and barriers have been shown to increase the IQE considerably [15] by suppression of the polarization

Journal Pre-proof

induced fields. The effects of QCSE can be moderated by use of very thin wells [16], and in this paper we follow this route by keeping the well widths to 5 Mono Layers (MLs).

In this paper, we focus on enhancing the IQE of GaN/AlN MQWs grown on sapphire substrates by PA-MBE through the modification of the growth parameters, without employing techniques for suppressing the dislocation densities or the internal electric fields.

2. Experimental Details

Growth of GaN/AlN MQWs was carried out in this work using a VEECO-Gen930 PA-MBE system using c-plane single side polished sapphire substrates (Monocrystal, Russia) of 2 inch diameter and 300µm thickness. The substrates were initially out-gassed in two different stages at 140 ºC and 400 ºC respectively. The deposition was carried out at 800 ºC. At first the substrate was exposed to active nitrogen which converted the top surface to AlN by nitridation process. The nitrogen plasma was activated using a Radio Frequency (RF) source from UNI-Bulb. The plasma power was kept at 400 W and the flow rate of the high purity (99.9999%) nitrogen gas used was 1.7 sccm. The plasma power was reduced to 350 W during the growth of subsequent epitaxial layers while keeping the other plasma parameters same. The plasma conditions were not changed further during the growth of subsequent epitaxial layers. On top of the nitridated substrate a ~40 nm thick AlN nucleation layer was deposited using a modified migration enhanced epitaxy (MEE) process [17]. The reflection high energy electron diffraction (RHEED) image obtained after the deposition of this layer was streaky indicating a relatively smooth surface. The Al flux was varied from 2.56×10^{-5} Pa to 2.97×10^{-5} Pa during the growth of this layer. Subsequently, a 500 nm thick AlN layer was deposited to improve crystal quality. During this growth a Ga flux was made incident to promote a smooth surface [18-19]. Twenty pairs of

Journal Pre-proof

Journal Pre-proof

GaN/AlN MQWs were grown on top of the AlN layer with Well and Barrier thicknesses of 5 MLs and 8 MLs respectively by keeping the Ga shutter on continuously and switching the Al shutter. A series of samples were grown by modifying the ratio of the group-III to group-V flux employed during the growth [20-21] and monitored using RHEED time evolution [22].

The excitation source used for the PL studies was a 10 mW He-Ag LASER (Photon Systems) emitting at 224 nm and a 100 mW He-Cd LASER (Melles Griot) emitting at 325 nm. For temperature dependent PL measurements the samples were mounted on to the cold finger of a 4 K cryostat (Cryo Industries of America, Inc.). A 9 KW Rigaku SmartLab X-Ray Diffractometer with rotating anode source was used for the High-Resolution X-Ray Diffraction (HRXRD) studies. A Zeiss Auriga Field Emission Scanning Electron Microscope (FESEM) system was used to study the surface morphology of the grown samples. An acceleration voltage of 3 kV was employed for these measurements. The Atomic Force Microscope (AFM) studies were carried out by a MFP-3D AFM system from Asylum Research with AFM probe from MikroMasch, Estonia.

Growth of III-Nitride materials by PA-MBE has been traditionally carried out under excess group-III regime [23] as smoother surface were obtained for these conditions of growth, and quantum well interfaces are typically controlled by the morphology of the underlying layers. Under such conditions of growth, the interface roughness was obtained to be near 1 ML, in the root mean squire (RMS) value [24]. However, the growth of AlN under excess group-III is complex, due to the very low desorption rates of Al at the growth temperatures employed. Near stoichiometric growth can lead to rough surfaces due to the short adatom mobilities. If an excess Al arrival rate is employed during growth, the un-reacted atoms stay on the growth surface due to low desorption rate, and may hamper further growth. There is therefore a very narrow window

Journal Pre-proof

where excess group-III conditions may be employed for AlN while avoiding these two extremes, which is difficult to maintain for long deposition times due to the natural drift of the effusion cell temperatures, plasma source parameters or substrate temperatures. A similar window between growth under Ga limited condition and the Ga droplet regime has been well documented in the literature, and is widens up for higher growth temperature [25]. However for AlN this is very narrow, due to the higher Al-N bond strength and the lower evaporation rates of Al when compared to Ga. A MEE process can be employed where the deposition under excess Al condition is carried out for a short period of time, followed by a plasma exposure step to consume the excess metallic atoms [26-28]. This was employed during the growth of the nucleation layer of the samples discussed in this work.

This process of switching of the effusion cell shutter every tens of seconds is unsustainable for thicker films and for long deposition times, and an alternative process was employed for growth of thicker AlN films in this work. The Al flux was chosen to be nearly stoichiometric, and the surface was exposed to an additional flux of Ga. As in case of stoichiometric growth of AlN all the active nitrogen are preferentially consumed by the arriving Al flux the un-reacted Ga does not incorporate into the film, but acts as a surfactant and increases the surface diffusion lengths of the Al adatoms. Since desorption rate of Ga is quite high at the growth temperature, this metallic Ga layer eventually evaporates.

3. Experimental Results

3.1 Growth by Plasma-Assisted Molecular Beam Epitaxy

We have investigated a series of samples in this work, whose schematic is shown in figure-1(a). The various layers include an AlN buffer layer grown using the MEE process explained

previously, an AlN film of ~0.5 µm thickness grown using Ga as a surfactant, and twenty GaN/AlN MQWs. The samples are nominally identical, except for the group-III to group-V flux ratio employed during growth. This parameter, which controls the diffusion length of surface adatoms, has been identified as very critical for control of surface morphology as well as incorporation of ambient impurities into the material [19]. However, it depends on several factors, including the arrival rates of Ga and Al, the efficiency of the RF plasma, the nitrogen flow rate and pumping rate of the chamber, as well as the substrate temperature which controls the desorption rate. It is difficult to control accurately all these parameters, but the group-III to group-V flux ratio can be determined relatively by deposition of a layer under excess group III for a time period T_{on}, and observation of the RHEED pattern. Since the additional metallic layer on the surface scatter the electron-beam, a dim and diffuse pattern is observed. However, if the surface is then exposed to the nitrogen plasma, there is a transition to a clear high-contrast pattern over a time period (T_{off}). The duration of this time period T_{off} is a direct measure of the group-III to group-V flux ratio, and can be used as a growth parameter [20-22].

As mentioned previously, during the growth of the MQW structure, the Ga as well as the nitrogen plasma shutter was kept on during both the well and barrier layer deposition, and the Al shutter was switched on and off. Therefore, Ga was present during the growth of the barrier layer, even though the incorporation is minimal due to the presence of the Al adatoms, which preferentially bond to the available active nitrogen. Unlike our recent work on AlGaN/AlGaN MQWs [4], no growth interruptions were carried out in between wells and barriers. A series of samples were investigated where the group-III to group-V flux ratio was varied from stoichiometric to excess group-III.

Journal Pre-proof

Figure-1(b) and 1(c) show the RHEED image of the sample surface after the growth of the AlN layer for one of the samples in the series as an example. These images were taken after leaving the sample at growth temperature of 800ºC to allow the excess Ga to evaporate. Streaky lines are observed, and clear (2×2) reconstruction lines are present both for the [1 1 -2 0] as well as the [1 0 -1 0] azimuths. This indicates both that the samples have the metal polarity, and that the overall surface is smooth.

3.2. Room Temperature Photoluminescence Measurements

Photoluminescence studies for a series of samples grown under varying group-III to group-V flux ratio were carried out at room temperature using a He-Cd LASER and the results are shown in figure-2(a). It can be observed that for all the samples the spectrum consists of a single peak. For samples grown under stoichiometric conditions, the peak is at 342 nm. As the group III/V flux ratio increases the PL peak continuously shifts to longer wavelengths, along with a near monotonic decrease in intensity. While initial studies as shown in figure-2(a) presents the experimental data for a series of samples with continually varying group III/V flux ratio, we have selected three samples for further study and determination of IQE values. The sample S1 was grown under excess group-III and shows a peak positioned at 355 nm, while the sample S3 was grown under nearly stoichiometric condition and shows the highest intensity and a peak at 344 nm, and the sample S2 has group-III/V ratio value between these two extremes and a peak at 350 nm.

Before determination of IQE, care was taken in the choice of LASER excitation to eliminate the possibility of band-filling and many-body effects. Hangleiter et al. has showed that for InGaN Single Quantum Well samples of well and barrier widths of 1 nm to 5 nm and 7 nm respectively, the probability of radiative recombination increases with the excitation power, thereby increasing

Journal Pre-proof

of IQE values [29]. Our excitation levels were deliberately kept low by employing a relatively large spot size of several mm square and such effects are not expected in our measurements. However, we have ensured this by carrying out room temperature PL studies as a function of excitation intensity using a set of optical density filters and the results are presented in figure-2(b). It was found that the PL intensity varies linearly with excitation levels as shown in figure-2(b). Moreover, the Full Width at Half Maxima (FWHM) of the PL peak was found to have only a minor variation with the change in excitation levels.

3.3. Temperature Dependent Photoluminescence Measurements

The direct measurement of IQE is complex and the well established technique for its estimation is through the ratio of PL intensity measured at room temperature to that measured at low temperatures [30-31]. We have investigated the samples S1, S2 and S3 by temperature dependent PL carried out using two different LASER sources, a He-Cd LASER emitting at 325 nm and a He-Ag LASER emitting at 224 nm. The second LASER has the advantage that the scattering is far from the wavelengths of interest. Furthermore, it establishes that these measurements are independent of excitation intensity and many-body effects are negligible.

The temperature dependent PL spectra for the sample S2 and S3 normalized to the maximum peak value in each case are presented in figure-3(a) and figure-3(b) respectively and the excitation wavelength used for these measurements was 224 nm. As shown previously there is a single peak at room temperature for both the samples and with cool down no additional peaks appear.

For sample S2, which was grown using moderate Ga coverage, the room temperature PL peak occurs at 355 nm and with cool down the peak shifts to a position of 347 nm at 4 K. For sample

Journal Pre-proof

S3, which was grown under stoichiometric conditions the corresponding peak positions are 344 nm and 341 nm respectively. The plot of peak intensity as a function of inverse temperature is presented in the inset for both samples. It is to be noted that for both the samples the peak shifts steadily to shorter wavelengths and no s-type behaviour is observed.

From the ratio of the room and low temperature PL peaks, we find that the IQE value for Sample S2 and S3 are 10% and 28% respectively. The IQE for S1, not shown here for limitation of space, is also nearly 10%. Figure-3(c) shows the values of the IQE for all three samples measured using the He-Cd and the He-Ag LASERs and while there is some scatter in the data, it was found that the values of IQE show a similar overall trend. This strong variation of IQE for very similar quantum well structures can be linked to a number of possible physical phenomena, and further investigations were carried out to identify their influence.

The improvement of the IQE can be due to the reduction of the dislocation density or may be due to generation of features that can localize the carriers away from the defect centeres leading to an increase in the radiative recombination probability. InGaN MQWs have extremely high IQE even at high dislocation densities. This phenomenon has been attributed to the presence of spinodal decomposition in these samples, which can lead to the presence of compositional inhomogenties [32-33]. This in turn leads to a fluctuation of the band-gap and can lead to localization of generated electron-hole pairs away from dislocations thereby increasing radiative recombination probability. AlGaN MQWs have also been shown to benefit from the presence of compositional inhomogeneities and high IQEs have been reported [34]. For GaN wells and AlN barriers, compositional inhomogenties do not occur and the source for localization of carriers can be linked to the nature of the well-barrier interface. The presence of pits in InGaN MQWs has been linked to the variation of the well and barrier widths and the creation of a potential barrier

surrounding the dislocations [35], which can also lead to a high IQE. To examine these possibilities the structural and surface morphological properties of these samples were studied and the results are given below.

3.4. X-Ray Diffraction of Quantum Wells

The samples were characterized by X-ray diffraction using an X-ray source with water cooled rotating copper anode. Cu K_α radiation (λ=1.54 Å) was used as the incident radiation in all the measurements. The measurements were carried out in a high-resolution mode that is employing a two-bounce Ge 220 monochromator in the incident path. The experimental configuration used a four-circle geometry with the sample placed on a horizontal stage, which can be rotated and tilted about its surface normal.

The θ-2θ plot of this X-ray diffraction study is shown in figure-4. For clear observation and distinct identification of the data corresponding to the three different samples, the observed X-ray intensity values are multiplied by constant numbers as indicated in the figure. The major peak observed in the graph occurs corresponding to AlN, indicating that despite the presence of the Ga flux, there was no incorporation of Ga in the bulk film for reasons explained previously. The MQW layers produce a series of peaks on either side of this main AlN peak, and their peak positions can be attributed to their periodic structure. It is clear that for all three samples, the peak positions are relatively similar. The peak at 35.1 º is the zeroth order of the superlattice (SL) structure, given by the average composition of the wells and barriers, as well as any residual strain.

The periodicity of the structures was determined by the equation given below:

Journal Pre-proof

$$P = \frac{\lambda}{2(\sin\theta_{n+1} - \sin\theta_n)} \quad \dots (1)$$

Where

P is the SL periodicity

λ is the wavelength of the incident X-ray (1.54 Å for Cu K_α line)

and θ_n is the peak position corresponding to the n-th order SL peak.

We find that the overall periodicity obtained from the three samples S1, S2 and S3 are 31.6 Å, 32.7 Å and 32.6 Å respectively, indicating a variation less than 1 ML. Since the growth rate remains the same for all layers, we can estimate the thickness ratio of the wells and barriers from their respective deposition times. From these two considerations, we can estimate that the wells and barriers were around 5 MLs and 8 MLs thick respectively. While the variation of periodicity is small, the nature of the interfaces, as indicated by the relative intensity and width of the SL peaks, show strong differences. The most prominent as well as the sharpest SL peaks were observed for sample S2, while for sample S1, grown under the highest Ga coverage, as well for sample S3, grown under stoichiometric conditions, the SL peaks were relatively weaker. The intensity of the SL peaks is linked to the quality of the interface, which includes both the abruptness of the interface - that is the presence of a clear transition between the well and the barrier - as well as the interface flatness. Since the samples were terminated at the end of the last barrier with no capping layer, we can estimate the nature of the interface roughness from the surface morphology, and our results of FESEM and AFM studies of the final surface are presented in the following section.

Journal Pre-proof

3.5. Surface Morphology

Journal Pre-proof

The surface of the samples S1, S2 and S3 were studied by FESEM with acceleration bias of 3 kV, and the images are produced in figure-5. Figure-5(a) shows the surface morphology of sample S1 which was grown under high Ga coverage. It can be observed that the surface is smooth with clear step-flow morphology. The flat regions observed are about 100 nm wide. With reduction of Ga coverage, the surface morphology is starkly different, and shows a reduction of size of the flat regions to about 30 nm, in the form of islands that are surrounded by a interconnected network of shallow trenches as can be observed for sample S2 in figure-5(b). The surface of sample S3 grown in the stoichiometric growth regime is given in figure-5(c) and show narrow ridge like features. Furthermore, we observe clear nano-dot like features decorating the top of the ridges. The diameters of these dots in the lateral direction are about 20 nm, with a relatively narrow size distribution.

In order to quantify the vertical dimensions, tapping mode AFM was carried out on the samples and the results are presented in figure-6. For sample S1, again flat step-like features were observed surrounded by pits which may be as deep as 5 nm. The flat surfaces exhibited an RMS roughness of 2 Å, while the overall image RMS was 7 Å. Similar RMS roughness was observed for S2. The dot like features observed in FESEM for sample S3 are again visible in the AFM image, which is presented in two different magnifications in figure-6(b) and 6(c). The ridge like features are observed in the AFM image with lengths around 200 nm and widths of 20 nm to 30 nm. The overall RMS roughness for this sample was increased significantly to 11 Å. Nano-dots decorate the top of the ridges and their widths and heights are about 20 nm and 2 nm respectively, indicating that they are disc-like in structure. It should be noted that a few of these dot like features are also observed for S1 and S2 samples, but their density is significantly lower.

Journal Pre-proof

The variation of surface morphology with the amount of Ga coverage can be linked to the surface diffusivity of the adatoms. It has been well established both experimentally as well as theoretically that the presence of a metallic adlayer on the growth surface allows the formation of a diffusion channel that increases the surface diffusivity of the adatoms and thereby reduces surface roughness. Both samples S1 and S2 were grown with a Ga adlayer on the surface and that leads to flat surfaces. The pits observed are typical of the termination of vertically propagating threading dislocations. The step flow morphology of sample S1 is a typical of MBE grown samples and is a result of a growth mode where active nitrogen is made incident on the growth surface coated with a layer of Ga. However the formation of nano-dots for growth under nearly stoichiometric conditions may be linked to the droplet-epitaxy related processes and is discussed in the next section.

4. Discussions

The formation of the nano-dots may have several mechanisms. The reduction of the Ga surface mobility can cause the formation of three dimensional structures by the Volmer Webber mechanism. However that is unlikely to generate dots of uniform sizes. The formation of strain induced islands has been reported in GaN quantum wells previously [36], but it is unlikely that only S3 will show this phenomenon and not the other samples which have the same thickness and composition of the wells and barriers. The third and more likely source is the formation of nano-droplets of Ga metal which then convert to GaN on exposure to active nitrogen. The thinness of the Ga coverage, along with the rough surface morphology can lead to formation of these nano-droplets through surface forces.

Journal Pre-proof

The effect of the growth mode on the density of threading dislocations, surface roughness and the internal quantum efficiencies observed have been summarized in table-1. Since in this work the focus has been on the improvement of the radiative recombination rate in MQWs using growth techniques and not from employment of various processes for reduction of dislocation densities such as interlayers or thick templates, we have left the AlN layer relatively thin. Thus, the dislocation densities as determined from on and off-axis rocking curves are quite high in all three films. We see a small reduction of the values in sample S3 and we believe it is related to the relatively rough surface morphologies. Such a growth mode tends to bend threading dislocations and cause their annihilation rather than allowing them to grow vertically and undiminished. We however would like to highlight the result that a relatively high value of IQE was observed even for relatively high dislocation densities. A number of reports in the literature have estimated the IQE for materials with such high dislocation densities and while there is a spread in the values, the predicted percentage numbers are very small, a result that is linked to the large number of non-radiative recombination centers associated with such defects.

While it is challenging to pinpoint the exact mechanism that leads to high IQE values even for samples with high dislocation densities, comparison of materials properties of samples S1, S2 and S3 does provide some indication. Our results indicate that for sample S1, even though the surface is the smoothest, the IQE is relatively low. This may be linked with the weaker XRD SL peaks, which indicate that when the growth is carried out under conditions of excess Ga coverage the interfaces are relatively diffuse and carrier localization is low. For samples S2 and S3 the interfaces are expected to be abrupt and not diffuse because the Ga coverage on the growth surface is either thinner or absent. This can be established from the relative increase of the SL

Journal Pre-proof

peaks of S2 compared to S1. However, even for this sample the IQE is relatively low, indicating that interface abruptness, while important, is possibly not a deciding factor.

The surface morphology of the sample S3 indicate a ridge-like nature, and this is typical of thin films of III-Nitride materials grown by MBE under near stoichiometric conditions. We believe that this roughness was established during the growth of the underlying layer and was replicated by the quantum wells deposited on top. The increased IQE therefore may be linked to the nature of the surface. The higher interface roughness is also indicated by the XRD results where the SL peaks are relatively weak and the higher orders are not clearly observable.

Based on these results, the strong increase of the radiative recombination probability can be linked to several causes. Firstly, the ridge-and-trench morphology suggests that the quantum wells are grown on planes which are tilted away from the [0 0 0 1] direction, and such structures will see a reduction of the QCSE. This will cause both an enhancement in luminescence efficiency as well as a blue shift in the peak. The shift to shorter wavelength was indeed observed for this sample. In addition, while the nanostructures observed on the growth surface are too large to act as quantum structures, they may play an important role in carrier confinement and thereby promote radiative recombination. A third possibility is the modification of the point defect density in the material due to a variation of Ga coverage on the growth surface. All of these effects come together to generate high IQEs despite the large dislocation density levels. While it is difficult to pinpoint the exact cause of the strong increase of IQE, in the absence of a strong reduction in dislocation densities, it is likely that all of these surface and interface features play a role in carrier localization away from non-radiative recombination centers. Since compositional inhomogeneity that is present in InGaN and AlGaN materials is absent in binary

Journal Pre-proof

GaN, this carrier localization effect can only be caused by confinement due to morphological reasons.

4. Conclusions

In this paper we have investigated methods to increase the IQE for GaN quantum wells. Since the alloy fluctuations as seen in AlGaN and InGaN structures are absent here, the carrier localization occurs solely through structural and morphological considerations. We observe that while a group-III-rich growth predictably leads to smooth surfaces, growth under stoichiometric conditions are more appropriate for optical emitters as the IQE values are significantly higher. This may be linked to a ridge-like surface morphology along with the presence of spontaneously formed nanostructures. Overall, we have observed IQE values of 28% for samples with dislocation densities near 10^{11} cm^{-2}. This can lead to a path where relatively efficient UV-LEDs can be developed on low cost substrates despite the presence of large dislocation densities.

Acknowledgements

This work was partially funded by the Department of Electronics and Information Technology (12(3)/2011-PDD), Government of India and by the Office of the Principal Scientific Advisor to the Government of India (Prn SA/W-UV LEDs/2017). Chirantan Singha would like to acknowledge the Department of Science and Technology (DST) INSPIRE fellowship (IF120257), Sayantani Sen (09/028(0921)/2014-EMR-I), and Alakananda Das (09/028 (0946)/2015-EMR-I) would like to acknowledge the Council of Scientific and Industrial Research (CSIR) Senior Research Fellowship scheme. Anirban Saha would like to acknowledge UGC for funding his work.

Journal Pre-proof

CRediT author statement

Chirantan Singha: Conceptualization, Methodology, Investigation, Writing - Original Draft. **Sayantani Sen:** Investigation. **Alakananda Das:** Investigation. **Anirban Saha:** Investigation. **Pallabi Pramanik:** Investigation. **Sudipta Bera:** Investigation. **Rupa Mukhopadhyay:** Validation, Supervision. **Anirban Bhattacharyya:** Conceptualization, Methodology, Validation, Writing - Review & Editing, Visualization, Supervision.

Declaration of interests

☑ The authors declare that they have no known competing financial interests or personal relationships that could have appeared to influence the work reported in this paper.

Journal Pre-proof

References

[1] Y. Wang, A. S. Özcan, K. F. Ludwig Jr., A. Bhattacharyya, T. D. Moustakas, L. Zhou, and D. J. Smith, Complex and incommensurate ordering in $Al_{0.72}Ga_{0.28}N$ thin films grown by plasma-assisted molecular beam epitaxy, Appl. Phys. Lett., 88, (2006) 181915.

[2] G. Coli, K. K. Bajaj, J. Li, J. Y. Lin, and H. X. Jiang, Excitonic luminescence linewidths in AlGaN alloys with high aluminum concentrations, Appl. Phys. Lett., 80, (2002) 2907.

Journal Pre-proof

[3] J. Zhang, H. Zhao, and N. Tansu, Effect of crystal-field split-off hole and heavy-hole bands crossover on gain characteristics of high Al-content AlGaN quantum well lasers, Appl. Phys. Lett., 97, (2010) 111105.

[4] S. Sen, C. Singha, A. Saha, A. Das, P. G. Roy, P. Pramanik and A. Bhattacharyya, AlGaN multiple quantum wells by PA-MBE for deep UV emission: Effect of growth interruptions, J. Cryst. Growth, 523, (2019) 125159.

[5] J. Han, M. H. Crawford, R. J. Shul, J. J. Figiel, M. Banas, L. Zhang, Y. K. Song, H. Zhou, and A. V. Nurmikko, AlGaN/GaN quantum well ultraviolet light emitting diodes, Appl. Phys. Lett., 73, (1998) 1688.

[6] V. N. Jmerik, D. V. Nechaev, A. A. Toropov, E. A. Evropeitsev, V. I. Kozlovsky, V. P. Martovitsky, S. Rouvimov, and S. V. Ivanov, High-efficiency electron-beam-pumped sub-240-nm ultraviolet emitters based on ultra-thin GaN/AlN multiple quantum wells grown by plasma-assisted molecular-beam epitaxy on c-Al_2O_3, Appl. Phys. Express, 11, (2018) 091003.

[7] M. Kneissl, T. Seong, J. Han and H. Amano, The emergence and prospects of deep-ultraviolet light-emitting diode technologies, Nat. Photonics, 13, (2019) 233.

[8] S. Y. Karpov and Y. N. Makarov, Dislocation effect on light emission efficiency in gallium nitride, Appl. Phys. Lett., 81, (2002) 4721.

[9] Q. Li, B. Li, L. Wang, Z. Zheng, B. Zhang, N. Liu, B. Li, M. Liu, Y. Huang, Z. Gong, Z. Chen, X. Liu, J. Luo and Z. Han, Comparison of 10 MeV electron beam radiation effect on InGaN/GaN and GaN/AlGaN multiple quantum wells, J. Luminescence, 210, (2019) 169.

Journal Pre-proof

Journal Pre-proof

[10] D. Fuhrmann, T. Retzlaff, U. Rossow, H. Bremers, A. Hangleiter, G. Ade, and P. Hinze, Large internal quantum efficiency of In-free UV-emitting GaN/AlGaN quantum-well structures, Appl. Phys. Lett., 88, (2006) 191108.

[11] M. Kneissl, T. Kolbe, C. Chua, V. Kueller, N. Lobo, J. Stellmach, A. Knauer, H. Rodriguez, S. Einfeldt, Z. Yang, N. M. Johnson, and M. Weyers, Advances in group III-nitride-based deep UV light-emitting diode technology, Semicond. Sci. Technol., 26, (2011) 014036.

[12] K. Takeda, F. Mori, Y. Ogiso, T. Ichikawa, K. Nonaka, M. Iwaya, S. Kamiyama, H. Amano, and I. Akasaki, Internal quantum efficiency of GaN/AlGaN-based multi quantum wells on different dislocation densities underlying layers, Phys. Status Solidi C, 7(7–8), (2010) 1916.

[13] O. Ambacher, J. Smart, J. R. Shealy, N. G. Weimann, K. Chu, M. Murphy, W. J. Schaff, L. F. Eastman, R. Dimitrov, L. Wittmer, M. Stutzmann, W. Rieger and J. Hilsenbeck, Two-dimensional electron gases induced by spontaneous and piezoelectric polarization charges in N- and Ga-face AlGaN/GaN heterostructures, J. Appl. Phys., 85 (6), (1999) 3222.

[14] M. Leroux, N. Grandjean, M. Laugt, J. Massies, B. Gil, P. Lefebvre and P. Bigenwald, Quantum confined Stark effect due to built-in internal polarization fields in „(Al,Ga)N/GaN quantum wells, Phys. Rev. B, 58 (20), (1998) 371.

[15] F. Wu, H. Sun, I. A. AJia, I. S. Roqan, D. Zhang, J. Dai, C. Chen, Z. C. Feng, and X. Li, Significant internal quantum efficiency enhancement of GaN/AlGaN multiple quantum wells emitting at ~350 nm via step quantum well structure design, J. Phys. D: Appl. Phys., 50, (2017) 245101.

[16] A. Bhattacharyya, I Friel, S. Iyer, T. C. Chen, W. Li, J. Cabalu, Y. Fedyunin, K.F. Ludwig Jr., T.D. Moustakas, H. P. Maruska, D.W. Hill, J.J. Gallagher, M.C. Chou and B. Chai, Comparative study of GaN/AlGaN MQWs grown homoepitaxially on (1 -1 0 0) and (0 0 0 1) GaN, J. Cryst. Growth, 251, (2003) 487.

[17] R. G. Banal, M. Funato, and Y. Kawakami, Characteristics of high Al-content AlGaN/AlN quantum wells fabricated by modified migration enhanced epitaxy, Phys. Status Solidi C, 7(7–8), (2010) 2111.

[18] J. Neugebauer, T. K. Zywietz, M. Scheffler, J. E. Northrup, H. Chen and R.M. Feenstra, Adatom Kinetics On and Below the Surface: The Existence of a New Diffusion Channel, Phys. Rev. Lett., 90(5), (2003) 056101.

[19] T. D. Moustakas and A. Bhattacharyya, Experimental Evidence that the Plasma-assisted MBE Growth of Nitride Alloys is a Liquid Phase Epitaxy Process, ECS Trans., 35(6), (2011) 63.

[20] P. Pramanik, S. Sen, C. Singha, A. S. Roy, A. Das, S. Sen, A. Bhattacharyya, D. Kumar and D. V. S. Rao, Controlling the compositional inhomogeneities in $Al_xGa_{1-x}N/Al_yGa_{1-y}N$ MQWs grown by PA-MBE: Effect on luminescence properties, J. Cryst. Growth, 439, (2016) 60.

[21] C. Singha, S. Sen, A. Das, A. Saha, S. Sikdar, P. Pramanik and A. Bhattacharyya, Spontaneous growth of III-nitride 1D and 0D nanostructures on to vertical nanorod arrays, Mater. Res. Express, 6, (2019) 1050b2.

[22] S. Sen, S. Paul, C. Singha, A. Saha, A. Das, P. G. Roy, P. Pramanik and A. Bhattacharyya, Monitoring the growth of III-nitride materials by plasma assisted molecular beam epitaxy employing diffuse scattering of RHEED, J. Vac. Sci. Technol. B, 38, (2020) 014007.

[23] J.I. Pankove, T.D. Moustakas, A Historical Survey of Research on Gallium Nitride, in: J. I. Pankove, T. D. Moustakas (Eds.), Semiconductors and Semimetals, Vol. 50, Elsevier, (1997), pp 1-10.

[24] Y. Cao, K. Wang, G. Li, T. Kosel, H. Xing and D. Jena, MBE growth of high conductivity single and multiple AlN/GaN heterojunctions, J. Cryst. Growth, 323, (2011) 529.

[25] B. Heying, R. Averbeck, L. F. Chen, E. Haus, H. Riechert, and J. S. Speck, Control of GaN surface morphologies using plasma-assisted molecular beam epitaxy, J. Appl. Phys. 88, (2000) 1855.

[26] G. Namkoong, E. Trybus, K. K. Lee, M. Moseley, W. A. Doolittle and D. C. Look, Metal modulation epitaxy growth for extremely high hole concentrations above 10^{19} cm^{-3} in GaN, Appl. Phys. Lett., 93, (2008) 172112.

[27] D. V. Nechaev, P. A. Aseev, V. N. Jmerik, P. N. Brunkov, Y. V. Kuznetsova, A. A. Sitnikova, V. V. Ratnikov, S. V. Ivanov, Control of threading dislocation density at the initial growth stage of AlN on c-sapphire in plasma-assisted MBE, J. Cryst. Growth, 378, (2013) 319.

[28] V. N. Jmerik, D. V. Nechaev, S. Rouvimov, V. V. Ratnikov, P. S. Kop'ev, M. V. Rzheutski, E. V. Lutsenko, G. P. Yablonskii, M. Aljohenii, A. Aljerwii, A. Alyamani, S. V. Ivanov, Structural and optical properties of PA MBE AlGaN quantum well heterostructures grown on c-Al_2O_3 by using flux- and temperature- modulated techniques, J. Mater. Res., 30(19), (2015) 2871.

Journal Pre-proof

[29] A. Hangleiter, D. Fuhrmann, M. Grewe, F. Hitzel, G. Klewer, S. Lahmann, C. Netzel, N. Riedel, and U. Rossow, Towards understanding the emission efficiency of nitride quantum wells, Phys. Stat. Solidi (a), 201(12), (2004) 2808.

[30] S. F. Chichibu, A. Uedono, T. Onuma, B. A. Haskell,A. Chakraborty, T. Koyama, P. T. Fini, S. Keller,S. P. Denbaars, J. S. Speck, U. K. Mishra, S. Nakamura,S. Yamaguchi, S. Kamiyama, H. Amano, I. Akasaki, J. Han and T. Sota, Origin of defect-insensitive emission probability in In-containing (Al,In,Ga)N alloy semiconductors, Nat. Mater., 5, (2006) 810.

[31] A. Getty, E. Matioli, M. Iza, C. Weisbuch, and J. S. Speck, Electroluminescent measurement of the internal quantum efficiency of light emitting diodes, Appl. Phys. Lett., 94, (2009) 181102.

[32] S. Chichibu, T. Azuhata, T. Sota, S. Nakamura, Spontaneous emission of localized excitons in InGaN single and multiquantum well structures, Appl. Phys. Lett., 69, (1996) 4188.

[33] S. Nakamura, The Roles of Structural Imperfections in InGaN-Based Blue Light-Emitting Diodes and Laser Diodes, Science, 281, (1998) 956.

[34] A. Bhattacharyya, T. D. Moustakas, L. Zhou, D. J. Smith, and W. Hug, Deep ultraviolet emitting AlGaN quantum wells with high internal quantum efficiency, Appl. Phys. Lett., 94, (2009) 181907.

[35] A. Hangleiter, F. Hitzel, C. Netzel, D. Fuhrmann, U. Rossow, G. Ade, and P. Hinze, Suppression of Nonradiative Recombination by V-Shaped Pits in GaInN/GaN Quantum Wells Produces a Large Increase in the Light Emission Efficiency, Phys. Rev. Lett. 95, (2005) 127402.

Journal Pre-proof

Journal Pre-proof

[36] N. Grandjean, B. Damilano and J. Massies, Group-III nitride quantum heterostructures grown by molecular beam epitaxy, J. Phys.: Condens. Matter 13, (2001) 6945.

Journal Pre-proof

Figure Captions

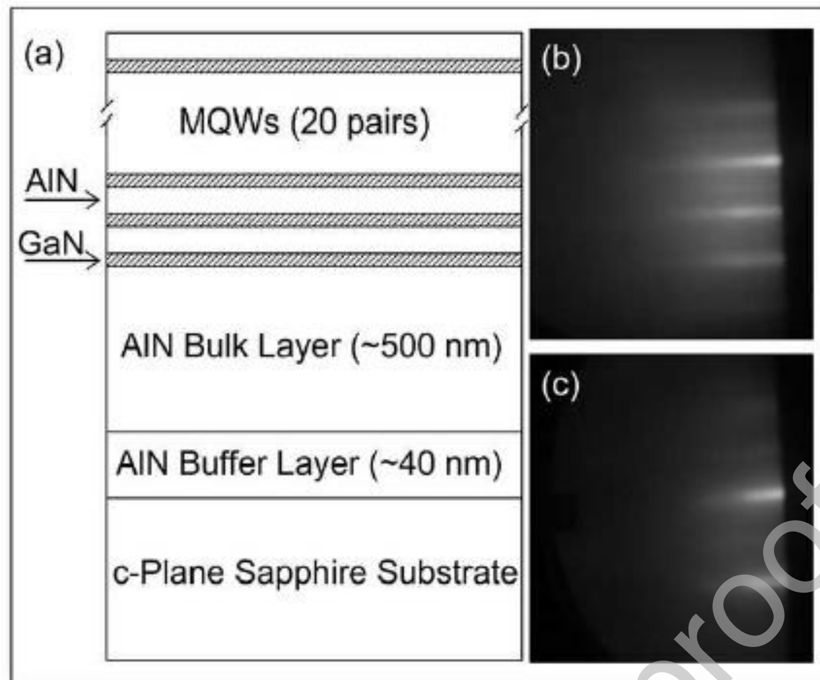

Figure-1: (a) Schematic of the samples, and RHEED for the [1 1 -2 0](b) and [1 0 -1 0](c) azimuths.

Journal Pre-proof

Journal Pre-proof

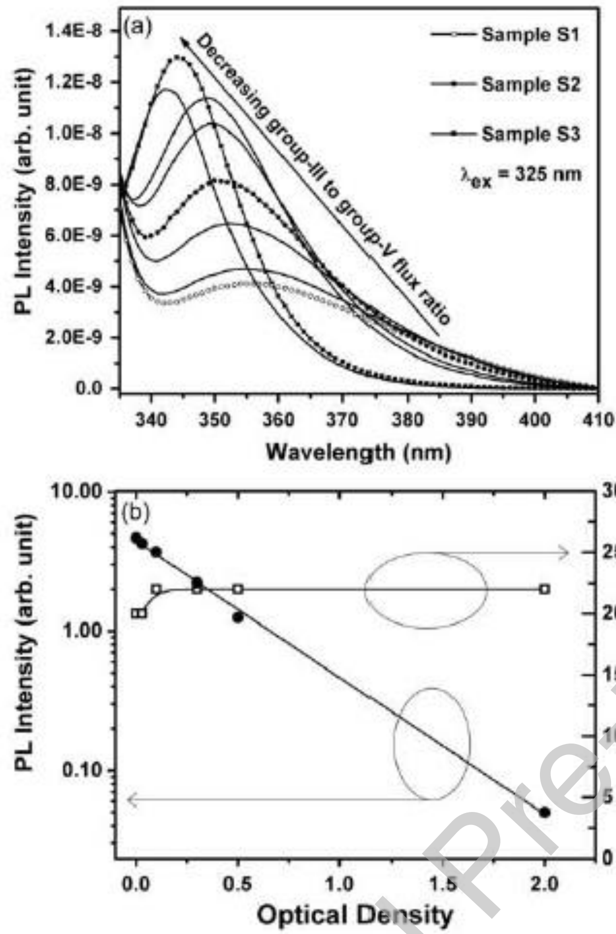

Figure 2: (a) Room Temperature PL spectrum of a series of samples with varying group III/V flux ratio, of which S1, S2 and S3 are indicated and (b) Variation of the PL intensity and the FWHM with Optical Density Filter for sample S3.

Journal Pre-proof

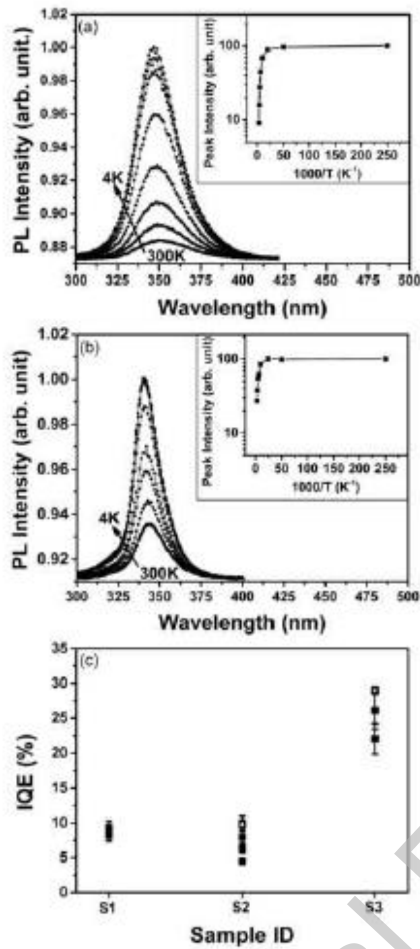

Figure-3: (a) Temperature dependent PL spectra (λ_{ex} = 224 nm) of sample S2 (normalized to the maximum peak). Inset: Plot of the PL intensity as a function of 1000/T for sample S2 (b) Temperature dependent PL spectra (λ_{ex} = 224 nm) of sample S3 (normalized to the maximum peak). Inset: Plot of the PL intensity as a function of 1000/T for sample S3 (c) IQE values of the three samples measured with the two different excitation sources.

Journal Pre-proof

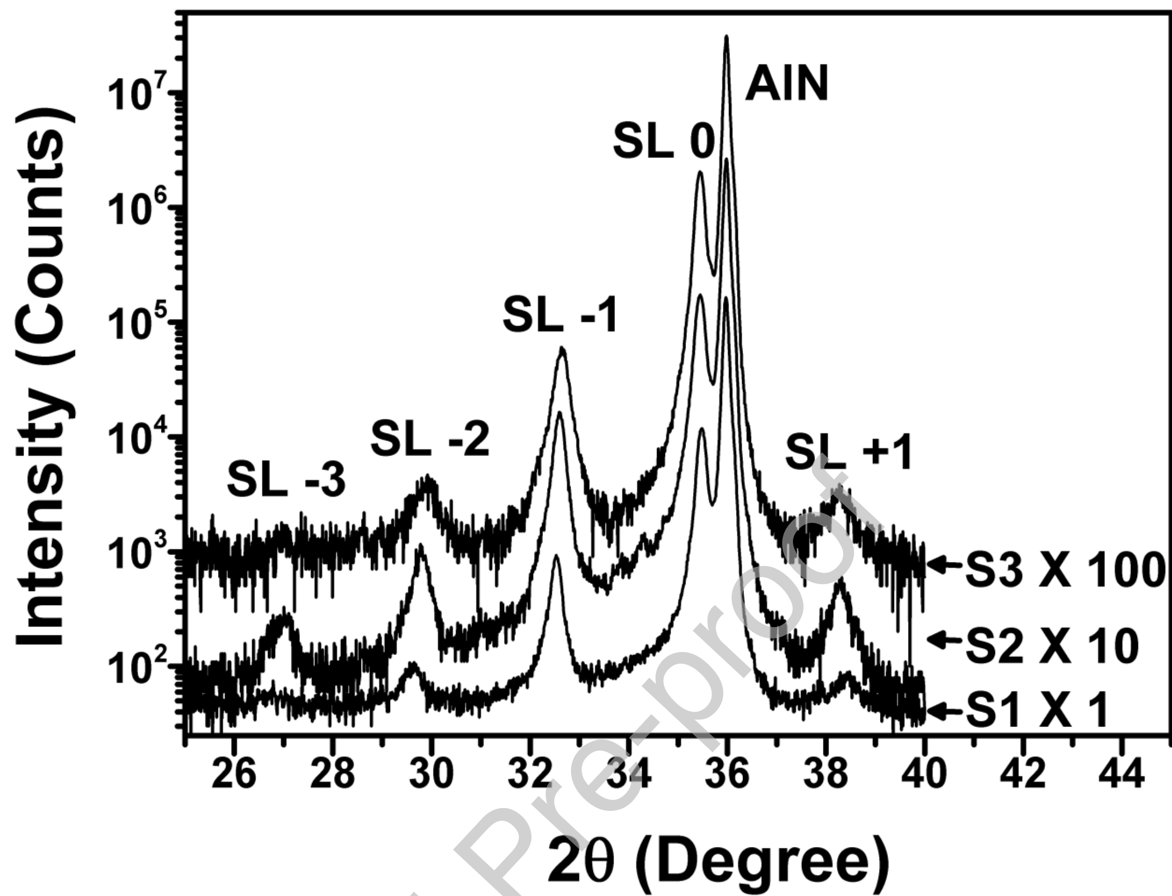

Figure-4: High Resolution X-ray θ-2θ plot of the three samples S1, S2 and S3.

Journal Pre-proof

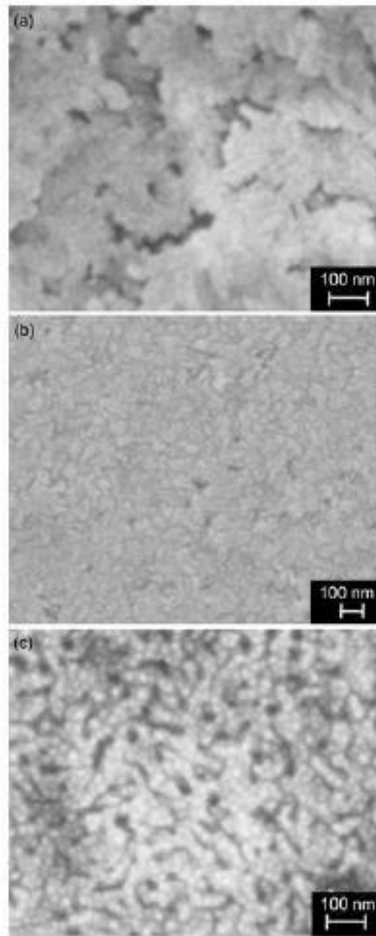

Figure-5: FESEM image of (a) sample S1 (b) sample S2 and (c) sample S3.

Journal Pre-proof

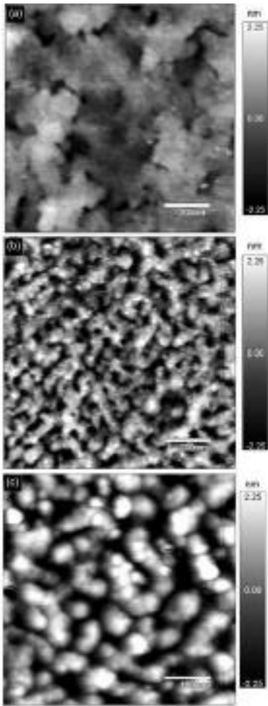

Figure-6: AFM images for sample S1 (a) and sample S3 (b) and (c) for area 1 μm x 1 μm and 500 nm X 500 nm respectively.

Journal Pre-proof

Table Captions

Table-1: Comparison of the dislocation densities, RMS roughness and IQE values of the samples.

Table-1

Sample ID	*Edge Dislocation density (cm^{-2})*	*Screw Dislocation density (cm^{-2})*	*RMS Roughness (Å)*	*IQE (%)*
S1	$1.2x10^{11}$	$1.1x10^{10}$	7	10
S2	$1.3x10^{11}$	$1.0x10^{10}$	7	~10
S3	$8.5x10^{10}$	$6.7x10^{9}$	11	28

Journal Pre-proof